# amorphous, glass and liquids

# Liquid Rb micrometric droplets confined in paraffin wax: an X-ray absorption spectroscopy study

**Simone De Panfilis,**[a]* **Andrea Di Cicco,**[a] **Adriano Filipponi,**[b] **Lucia Comez**[a] **and Michael Borowski**[c]

[a]*I.N.F.M. and Dip. di Matematica e Fisica, Università di Camerino, I-63032 Camerino (MC), Italy,* [b]*I.N.F.M. and Dip. di Fisica, Università dell'Aquila, I-67010 Coppitto (AQ), Italy, and* [c]*E.S.R.F., B.P. 220, F-38043 Grenoble, France. E-mail: depa@unixas.unicam.it*

We have performed high-quality X-ray absorption measurements on crystalline (c-Rb) and liquid ($\ell$-Rb) Rubidium in the range from 15 K to 320 K. Performing a consistent analysis that takes into account the contribution of the medium range structure, we observe that the $\ell$-Rb spectrum is compatible with pair correlation function $g(r)$ previously determined by neutron diffraction experiments. Due to the micrometric size of the liquid droplets we were able to observe a slight undercooling down to 290 K. We were also able to study the details of the very strong multielectron excitations channels in terms of resonances, edges and shake-off features at proper theoretical energy values.

**Keywords: liquid metals**; **multielectron excitations**; **X-ray absorption spectroscopy.**

## 1. Introduction

Liquid alkali metals present very intriguing static and time-dependent properties, among which the possibility to describe the interatomic interactions with a potential model, whose functional form is universal for all these elements under appropriate scaling (Price *et al.*, 1970, Balucani *et al.*, 1993). But the local atomic arrangement is tightly related to shape of the repulsive part of the interatomic potential. It is then evident that an exact experimental determination of the finest details of the pair correlation function $g(r)$ is fundamental to correctly cast the theoretical potential parameters.

The X-ray absorption spectroscopy (XAS) is a powerful tool in the structural study of liquids (Crozier *et al.*, 1988). In the last few years, because of its intrinsic short range sensitivity, XAS has been proved to be extremely useful in refining the very first peak shape of the pair correlation function of liquids determined by x-ray (XRD) or neutron (ND) diffraction measurements (Di Cicco & Filipponi, 1994, Di Cicco *et al.* 1997, Filipponi *et al.*, 1999). In many cases it may be difficult to probe the reciprocal space in the high $q$ range by diffraction experiments indeed, and this represents a crucial limiting issue to the resulting resolution in the real space.

When measured near the melting point $T_m$, liquid alkali metals also provided a realistic benchmark for the simplified mode-coupling theories which have been developed in the last decades (for a review see: Götze & Sjögren, 1992 ). But still it is an open issue how these theories describe the dynamical behaviour of these simple liquid metals when they are cooled well below the melting point, down to an undercooled metastable phase. The high chemical reactivity of pure alkali elements creates severe constraints while running the experiments, and this strongly limits the scientists in getting a better insight in the structural and dynamical behaviour of undercooled liquid phases. Conventional techniques which allow to study undercooled liquids (drop-tubes, levitation apparatus) are very difficult to be run in the case of alkali metals, as these may require sealed sample environments.

In the present paper we report a XAS study of crystalline and liquid Rubidium. Furthermore, following the technical ideas successfully applied in previous studies which coupled the XAS to the study of the structure and the nucleation mechanism of undercooled liquid phases (Di Cicco, 1997, Filipponi *et al.*, 1999, Pascarelli *et al.*, 2000, De Panfilis & Filipponi, 2000), we were able to observe a slight undercooling of about 20 K below the melting point $T_m$.

## 2. Experimental and results

The Rb $K$-edge XAS measurements have been performed at the BM29 beamline spectrometer of the European Synchrotron Radiation Facility using a Si$<$311$>$ double crystal monochromator (Filipponi *et al.*, 2000). XAS spectra of the liquid and solid Rb where recorded in transmission mode using Ar filled ionization chambers. The simultaneous detection of a RbI reference sample at room temperature downstream to the experimental specimen was used to check the energy stability to be better then 0.05 eV along the entire run of measurements. The low-temperature XAS measurements have been performed cooling the sample in a closed-cycle cryostat able to scan the temperature range $13 - 400$ K. The sample holder is decoupled from the vibrating cold-head in order to minimise the sample displacements during the absorption measurement.

Due to the high corrosivity of both solid and liquid Rb, it was necessary to confine the sample in a sealed sample holder, avoiding any contact with oxygen or moisture. At the same time, transmission XAS experiments require a high transparency of the sample holder walls. Moreover, the optimal Rb thickness required to maximise the signal-to-noise ratio is smaller than 80 $\mu$m, and this just add further impediments in the sample preparation.

The sample suitable to overcome to all these difficulties was produced following a protocol lent by a well established procedure valid for high-temperature studies (Filipponi *et al.*, 1998). Micrometric size Rb grains (99.6% purity) were mixed in 1:20 weight dilution with an inert oxygen and moisture free paraffin wax, whose melting point was higher than the Rb one. This was achieved by emulsionating the liquid Rb and wax in an Ar atmosphere oxygen-free glove-box by a steering apparatus. The emulsion was then poured into a PFTE rectangular cavity of about 2 mm thickness, provided with a steel screw-cap and a viton sealing gasket. This sample holder was then coupled with a *Pt100* temperature sensor and installed into the cryostat chamber.

Because of the micrometric dimension of the Rb droplets dispersed in the paraffin wax, we were able to observe a slight undercooling of about 20 K, as evidenced by the differential absorption $\delta\alpha(T) = \alpha(T;E_1) - \alpha(T;E_2)$ temperature scan (Filipponi *et al.*, 1998) shown in the upper panel of Fig. 1. The presence of a hysteresis loop demonstrates the undercooling of the liquid Rb sample. The occurrence of a sharp transition at the melting point $T_m = 312$ K is characteristic of a high-purity sample, demonstrating the absence of any possible chemical reaction occurred between the Rb and the wax.
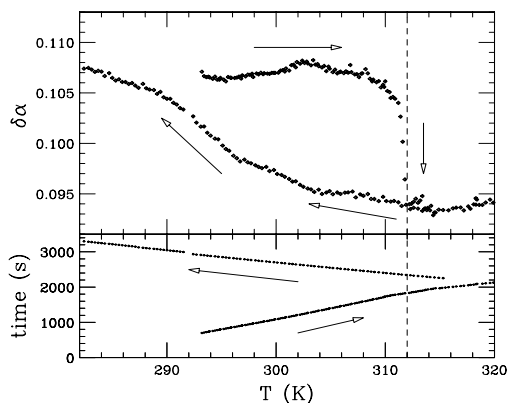
**Figure 1**
Upper panel: differential absorption $\delta\alpha$ as a function of the temperature taken at $E_1 = 15.2035$ keV and $E_2 = 15.2083$ keV; the hysteresis cycle shows a sharp transition at the melting point $T_m = 312$ K (dashed line), and a smoother freezing pattern during the cooling stroke. Lower panel: thermal history of the Rb sample while recording the temperature scan.

As it has been pointed out in many papers, a proper analysis of the X-ray absorption fine structure (XAFS) in a XAS experiment can not skip over the fundamental step of a careful determination of the atomic background over which the XAFS signal is superimposed (D'Angelo *et al.*, 1995, Filipponi & Di Cicco, 1995). Usually, this is accomplished either by heuristic automatic routines which minimise the contribution of the low frequencies in XAFS signal (Li *et al.*, 1992), or by adding edge-like analitycal contributions, to which it is then possible to attribute a physical meaning.
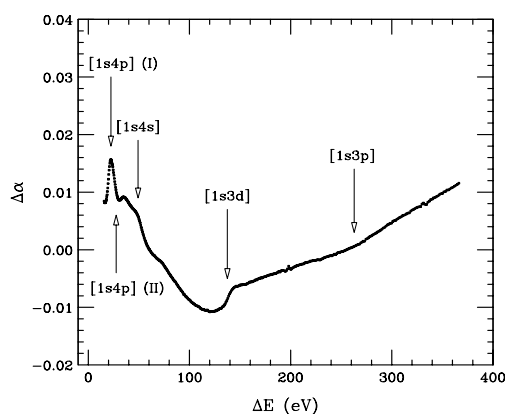


**Figure 2**
Absorption K-edge excess $\Delta\alpha$ as a function of the energy above the threshold $E_0 = 15.2026$ keV in liquid Rb. Arrows mark the calculated energy thresholds for the inner-shell events which involve the simultaneous double excitations of the 1*s* and 4*p*, 4*s*, 3*d* or 3*s* electrons, respectively.

Rb is well known to show an atomic background affected to a high degree by anomalies associated with the opening of multi-electron excitation channels (Kodre *et al.*, 1997). This is evident in Fig. 2 where we present the *K*-edge absorption excess $\Delta\alpha$ of liquid Rb after the subtraction of an average linear decay, normalized to the *K*-edge discontinuity. In this case, due to the extreme weakness of the XAFS signal in liquid Rb, the most evident features visible in $\Delta\alpha$ corresponds to the onset of the double-electron excitations. It

is then evident that a correct approach to extract a weak but meaningful XAFS signal requires a strong bias on a physical basis. The arrows in Fig. 2 indicates the energy thresholds for the shake-up channels leaving the double-hole [1*s*4*p*], [1*s*4*s*], [1*s*3*d*] and [1*s*3*p*], calculated using a relativistic atomic self-consistent scheme (Filipponi & Di Cicco, 1995). The [1*s*4*p*] was resolved in a shake-up (*I*) and shake-off (*II*) channels.

For the precision required in the XAFS data analysis, double-electron excitations can be very well described in terms of simple functional forms (Filipponi *et al.*, 1995). However, for the most inner shells a more complete analysis can be performed in order to obtain a better agreement with theoretical estimates (Schaphorst *et al.*, 1993). In particular, it has been showed that each double-electron channel can be decomposed in a combination of a double bound-bound resonance, a shake-up edge and a shake-off brake of slope. In Fig. 3 we present such a decomposition for the [1*s*3*d*] and [1*s*3*p*] double electron features, where we show that it is the presence of a small resonance which causes an apparent shift of about 20 eV of the experimental data with respect to the calculated energies of the shake-up excitations reported in Table 1.

**Table 1**
Differences of total energy required to create additional core holes in the isolated atom based on a relativistic self-consistent theory (Filipponi & Di Cicco, 1995).

|  | [1*s*3*d*] | [1*s*3*p*] |
|---|---|---|
| $\Delta E$ (eV) | 138.5 | 274.5 |
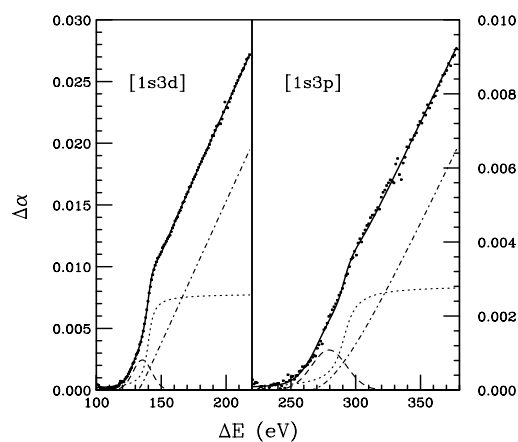


**Figure 3**
Theoretical decompositions of the [1*s*3*d*] (left) and [1*s*3*d*] (right) multielectron photoexcitation features in the absorption spectrum of liquid Rb: resonance (dashed line), edge (dotted line) and shake-off (dot-dashed line); the bullets are the experimental data and the relative absorption is normalized to the overall discontinuity jump at the K-edge.

Solid Rb XAFS signals $\chi(k)$ have been analysed within the GNXAS data analysis framework (Filipponi *et al.*, 1995), including 2-body and, where appropriate, 3-body terms. Anharmonic effects in the crystalline Rb spectra have been taken into account by means of asymmetric coordination shells. An example of the best fit procedure result is shown in Fig. 4.a for the 15 K case. The atomic background which accounts for the aforementioned multielectron excitations as been kept fixed and equal to the one determined for the liquids. The $S_0^2$ parameter was let free to vary while fitting the spectrum collected at the lowest temperature, when the

coordination numbers and the distances of the different coordination shells were fixed to their respective crystallographic values. In all the other cases it was kept fixed to this value.

Liquid Rb measurements have been treated following a consistent data analysis method (A. Filipponi, 1994) that takes into account long-range asymptotic behaviour contained in a $S(q)$ previously measured by neutron diffraction (Balucani *et al.*, 1993). The resulting best fit for the liquid at 320 K is presented in Fig. 4.b.

In this case, because of the relatively large average distance of the first neighbours (the first peak in the $g(R)$ of liquid Rb has a maximum at $R = 4.85$ Å) and because of the intrinsic high degree of the structural disorder, the efficiency of the photoelectron backscattering is largely dumped and the 2-body signal is very weak.
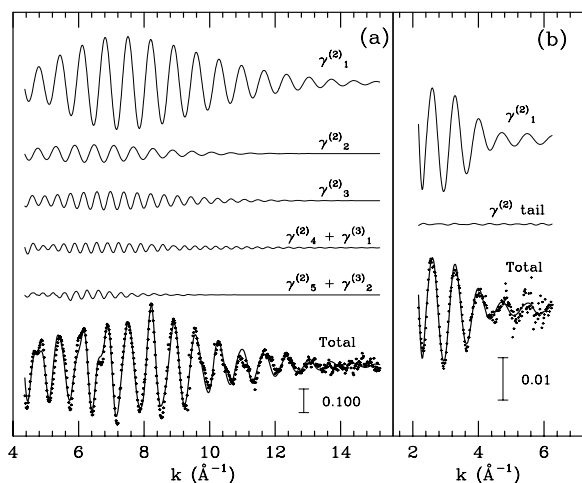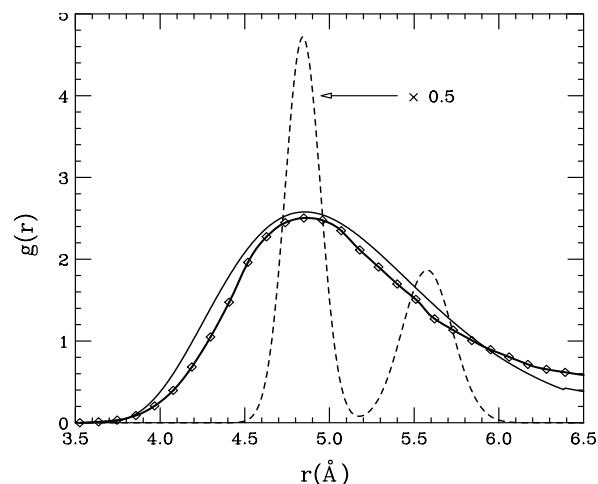


**Figure 4**
 Best fit (continuous line) of experimental $k^2 \chi(k)$ data (points) at 15 K (a) and 320 K (b). The signals associated with the relevant 2-body ($\gamma^{(2)}$) and 3-body ($\gamma^{(3)}$) paths are also shown. In the case of the liquid Rb, the contribution of the long-range 2-body tail from a ND experiment is also presented.

The reconstructed pair correlation functions $g(r)$ for solid (at $T = 15$ K) and liquid Rubidium as determined by our XAFS measurements are presented in Fig. 5, where we also plot the model $g(r)$ from the ND experiment.

## 3. Concluding remarks

The present study shows the potential of a careful XAS investigation on a mono–atomic system. We demonstrated the possibility to cool liquid Rb into a metastable undercooled liquid phase, down to 290 K. Furthermore, we remarked the importance to properly account for multi-electron excitation features in the determination of the atomic background over which the XAFS signal is superimposed. In the case of liquid Rb, the most intense shake-up resonance was found to be ten times larger than the amplitude of the XAFS oscillations. A proper analysis of the double-electron excitations have been carried on for the [1s3d] and [1s3p] double-hole in terms of functional decomposition of the different innershell excitation components. This proved that a perfect agreement with theoretical self-consistent calculation can be achieved when one take into account a small resonance which cause an apparent shift of the excitation threshold.



**Figure 5**
 Reconstructed $g(r)$ for solid at 15 K (dashed line, times 0.5 for clarity) and liquid at 320 K (solid line). The diamond symbols track the model pair correlation function determined by the ND measurement.

The $\chi(k)$ XAFS signals for solid and liquid Rb have been fitted within the GNXAS framework and the relative structural parameters where in agreement with the crystallographic data and with the pair correlation function previously determined by ND experiments.

Experiments have been performed at the ESRF-BM29 beamline during beamtime allocated for the proposals CH-783. We acknowledge Dr. H. Müller for the useful assistance while running the glove-box during the sample preparation.

## References

U. Balucani, A. Torcini & R. Vallauri (1993). *Phys. Rev. B* **47**, 3011–3020.

E. D. Crozier, J. J. Rehr & R. Ingalls (1988), in *X-ray Absorption*, edited by D. C. Konigsberger & R. Prins, pp. 373–442, New York: J. Wiley & Sons.

P. D'Angelo, A. Di Nola, E. Giglio, M. Mangoni & N. V. Pavel (1995). *J. Phys. Chem.* **92**, 2858–2865.

S. De Panfilis & A. Filipponi (2000). *J. Appl. Phys.* **88**, 562–570.

A. Di Cicco & A. Filipponi (1994). *Europhys. Lett.* **27**, 407–412.

A. Di Cicco, M. Minicucci & A. Filipponi (1997). *Phys. Rev. Lett.* **78**, 460–463.

A. Di Cicco, (1998). *Phys. Rev. Lett.* **81**, 2942–2945.

A. Filipponi (1994). *J. Phys.: Condens. Matter* **6**, 8415–8427.

A. Filipponi & A. Di Cicco (1995). *Phys. Rev. A* **52**, 1072–1078.

A. Filipponi, A. Di Cicco, & C. R. Natoli (1995). *Phys. Rev. B* **52**, 15122–15134; **52**, 15135–15145.

A. Filipponi, M. Borowski, P. W. Loeffen, S. De Panfilis, A. Di Cicco, F. Sperandini, M. Minicucci & M. Giorgetti (1998). *J. Phys.: Condens. Matter* **10**, 235–253.

A. Filipponi, A. Di Cicco, & S. De Panfilis (1999). *Phys. Rev. Lett.* **83**, 560–563.

A. Filipponi, M. Borowski, D. T. Bowron, S. Ansell A. Di Cicco, S. De Panfilis, & J.-P. Itiè (2000). *Rev. Sci. Instrum.* **71**, 2422–2432.

W. Götze & L. Sjögren (1992). Rep. Prog. Phys. **55**, 241–376.

A. Kodre, I. Arčon, & R. Frahm (1997). *J. Phys. (France)* **7**, 195–197.

G. Li, F. Bridges & G. S. Brown (1992). *Phys. Rev. Lett.* **68**, 1609–1612.

S. Pascarelli, S. De Panfilis & T. Neisius (2000). *Phys. Rev. B* **62**, in press.

D. L. Price, K. S. Singwi & M. P. Tosi (1970). *Phys. Rev. B* **2**, 2983–2999.

S. J. Schaphorst, A. F. Kodre, J. Ruscheinski, B. Crasemann, T. Åberg, J. Tulkki, M. H. Chen, Y. Azuma & G. S. Brown (1993). *Phys. Rev. B* **47**, 1953–1966.